



Polyaniline Emulsion as a Passivator in Styrene-Acrylate Waterborne Coatings for the Protection of Carbon Steel against Corrosion



Samir M.M. Morsi^{1*}, Lobna A. Khorshed², G.N. Samaan³, S. Sobhi⁴, E.F. Abadir⁴, A.I. Hussain¹

¹Polymers and Pigments Dept. National Research Centre, Dokki, Giza, Egypt.

²Physical Chemistry Department, National Research Centre, Dokki, Giza, Egypt.

³International Trade Agencies and Marketing Corporation (ITAMCO), Egypt.

⁴Department of Chemical Engineering, Faculty of Engineering, Cairo University, Egypt.

THE passivation effect of polyaniline (PANI) was utilized to enhance the protection efficiency of styrene-acrylate waterborne coatings against corrosion of carbon steel (CS). Styrene-acrylate emulsion (SACE) based on poly (styrene-co-butyl acrylate) was synthesized via a semi-batch emulsion polymerization while the PANI emulsion (PANE) was prepared by chemical oxidative polymerization of aniline in the micelles of sodium dodecyl benzene sulfonate. The coating formulations (Fs) were prepared by adding PANE to SACE at different weight solid ratios. The viscosity, density, solid content, particle size distribution, the shape of the particles, and stability of the blended emulsions were studied. The properties of the coated-films were evaluated such as hardness, impact resistance, flexibility, adhesion to the steel, glass transition temperature (T_g), and surface morphology. The effect of PANE in enhancing the protection efficiency of SACE film against corrosion of CS was estimated by visual corrosion test, weight loss measurements, and electrochemical Tafel polarization. The results showed an increase in the T_g from 23 °C for pure SACE film up to 36 °C for the film containing the maximum PANI content. SACE film loaded with 0.75% and 1% PANI exhibited the least corrosion current density of 0.07 and 0.11 μA/cm², respectively. The formation of a passive layer on the coated-CS was recorded by the shift of corrosion potential for steel to the anodic direction.

Keywords: Styrene acrylate, Polyaniline emulsion, Corrosion protection, Steel, Eco-friendly coatings.

Introduction

The problem of steel corrosion is one of the most important problems faced by all countries of the world and threatens the infrastructure, economy, pipelines, bridges, buildings, aircraft, household electrical appliances, and others. Organic coatings are the most common methods used to protect steel structures especially solvent-based coatings [1-3]. However, they are environmentally harmful. PANI is also used in the corrosion protection of steel substrates due to its passivation effect [4].

Styrene-acrylate copolymers are milky-white water-based emulsions that are built-up from styrene and various acrylic monomers such as butyl acrylate, acrylic acid, methyl methacrylate, etc. Their solid is ranged from 40% to 60% by weight with an ammonia or acrylic odor. They are used in a variety of industrial and consumer end-use applications such as; secondary binder in glass fiber reinforced wall covering panels, floor and ceramic tile adhesive, elastomeric roof coatings, wall putties, architectural decorative coatings, concrete membrane applications,

*Corresponding author e-mail: samirmchemist@gmail.com

Received 28/3/2019; Accepted 7/5/2019

DOI: 10.21608/ejchem.2019.11251.1724

© 2019 National Information and Documentation Center (NIDOC)

cement mortar and concrete additives, and soil stabilizers. They are manufactured by mixing liquid styrene and acrylic monomers in water. The mixed-monomers are emulsified with ionic and/or non-ionic surfactants to form a stable monomer-in-water suspension. A polymerization reaction is proceeded by a free-radical initiator and the monomers react to form styrene-acrylic copolymers that remain in a stable emulsion form [5,6].

PANIs are semi-conductive polymers that possess a π -conjugated system extended along their backbone. They acquire their electrical conductivity by a process known as "doping". Their advantages over other conductive materials are their easy preparation, light-weight, flexibility, resistance to corrosion, low cost, stability, affordability, and redox properties [7,8]. They can be tailor-made to the required application such as antistatic coatings, batteries, thin film transistor, electromagnetic shielding, artificial muscles, light-emitting diodes, biosensors, fuel and solar cells, fillers, corrosion protective coatings, etc [9]. However, despite the physical and mechanical properties of PANI that are acquired from their high aromatic nature and intermolecular hydrogen bonding between the adjacent chains, the use of PANI is restricted on their solid form. This is because of their poor solubility, brittleness, and unprocessable nature. Three methods have been used to improve the solubility and processability of PANI by structure substitution, copolymerization, and synthesis of PANI by emulsion polymerization. However, the conductivity of the material is affected in the first two methods. Therefore, the latter method is considered the most profitable. An emulsifier is used in the emulsion polymerization of PANI to enhance the molecular weight of the polymer by affecting the locus of polymerization and to stabilize the colloidal form of the polymer. Therefore, the obtained emulsified PANI has good solution processability, high molecular weight, and good electrical conductivity [10].

Lamouri and Zeghina [11] prepared a styrene copolymer with 30 % of acrylic acid and formulated composites with concentrations of PANI ranging from zero to 30 wt %. They studied the morphological and electrical properties of the composites. Wu *et al.* [12] used poly (maleic anhydride-co-acrylic acid-co-sodium p-styrenesulfonate) to stabilize PANI/polyacrylate composite emulsions.

Egypt.J.Chem. **62**, No. 11 (2019)

In this regard, we aim through this paper to prepare both styrene-acrylate and PANI emulsions and mix them in this water-based form. The blended emulsions were used as coating formulations and applied on steel substrate to study their anticorrosive properties as environmentally friendly coatings.

Experimental

Materials

Styrene (St), butyl acrylate (BA), acrylic acid (AA), and aniline (AN) were obtained from Sigma-Aldrich. These monomers were distilled in a rotary evaporator under reduced pressure before use and stored at -20 °C. Acrylamide (AAm), sodium bicarbonate (NaHCO_3), ammonia, and potassium persulfate (KPS) were supplied from Sigma chemicals. Sodium dodecyl benzene sulfonate (SDBS) and nonylphenol ethoxylate (NP30) were obtained from Sigma-Aldrich and DOW Chemical, respectively. Texapon® N70 was supplied from BASF Company. Acetic acid (AcAc) was supplied by El-Nasr Pharmaceutical Chemicals Co., Egypt.

Methodology

Synthesis of styrene acrylate emulsion (SACE)

Three containers were used to prepare the SACE by a semi-continuous seeded polymerization method [13,14]. The first reactor container includes 30 ml distilled water, 2.18 g NP30, 0.30 g KPS, and NaHCO_3 as a buffering agent. This container was heated up to 80-83°C with continuous stirring. The second pre-emulsion container includes 60 ml distilled water, 1.45 g Texapon N70, and a mixture of monomers including 43.43 g (417 mmol) St, 47.16 g (368 mmol) BA, 3.63 g (50.4 mmol) AA and 0.54 g (7.6 mmol) AAm. This container was stirred with a high-speed homogenizer (ultra turax homogenizer) for 30 min at ambient temperature. The third initiator container includes 0.15 g KPS dissolved in 10 ml distilled water. The second container was dosed to the first reactor container over 3.5 h while the initiator container was dosed to the reactor over 4 h. After which, the reaction was allowed to proceed for an additional 1 h at 80 rpm. Then, the temperature was cooled gradually to 40 °C over 1h. The pH was adjusted to 8 using an aqueous solution of ammonia and the product was filtered over 200-micron nylon sock. The solid content of the produced emulsion is ~ 51.1%. The chemical structure of the prepared styrene-acrylate copolymer is presented in **Fig. 1**.

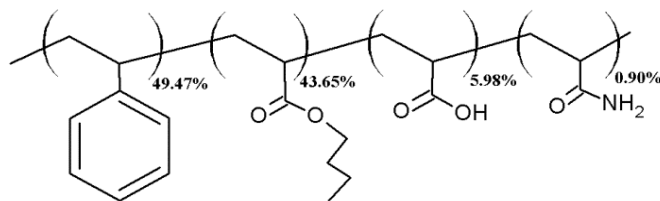


Fig. 1. The suggested structure of styrene-acrylate copolymer.

Synthesis of polyaniline emulsion (PANE)

PANI was synthesized by chemical oxidative method [15] in an emulsified form to prepare a processible conducting PANI. 13.07 g (0.0375 mol) SDBS was poured to round flask containing 50 ml distilled water and equipped with a mechanical stirrer. 2.33 g (25 mmol) AN was added to the flask with continuous stirring. The initiator solution was prepared by dissolving 3.379 g (12.5 mmol) KPS in 125 g distilled water and added drop by drop during 30 min to the reaction flask. Finally, 3.75 g (62.5 mmol) AcAc was added to the flask. The reaction mixture was left stirring at room temperature for 24 h. The solid content of the produced emulsion is ~ 18%.

Synthesis of coating formulations

Six coating formulations (Fs) were prepared by mixing the prepared SACE and PANE by stirring at 80 rpm. **Table 1** lists the amount of SACE and PANE included in the prepared Fs and **Fig. 2** shows the prepared Fs and PANE.

Characterization techniques

Analytical tests

Differential scanning calorimetry analysis (DSC) was recorded on TA Instruments DSC Q20 V24, 11 build 124. All samples were heated with a scan rate of 10 °C/min over a temperature range of 0 °C to 50 °C under a nitrogen atmosphere. The particle size of the CBs and their distribution pattern were determined by dynamic light scattering (DLS) in the range of 0.4–10,000 nm using Malvern Zetasizer nano, UK. High-Resolution JEOL-2100 TEM and Quanta FEG-250 SEM instrument, Ametek Holland, were used to obtain transmission and scanning electron micrographs, respectively.

Physical and mechanical tests

The viscosity was measured according to *ASTM D2196-10, 2010* using a digital viscometer manufactured by Sheen Company. The solid

content (S.C.) was calculated as the average of three experiments according to *ASTM D4209-07, 2013*.

$$\text{S.C.} = \frac{W_i}{W_o} \times 100$$

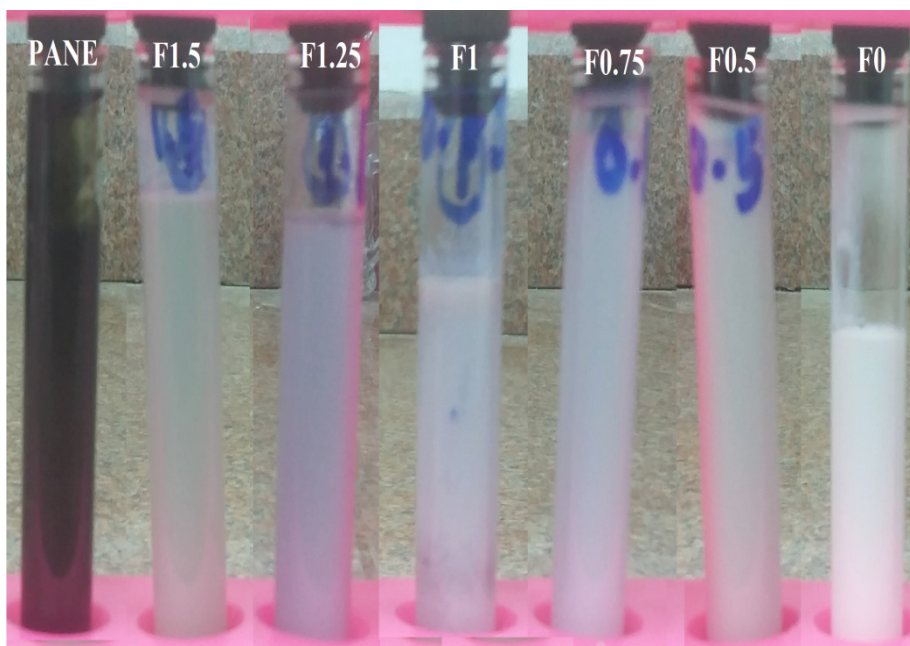
where W_i is the final weight of the sample after drying and W_o is the initial weight of the sample. The prepared coating formulations were applied on metal or glass panels by using a film applicator to obtain an appropriate and uniform dry film thickness. The adhesion of the prepared dry films to the metal substrate was evaluated using a cross-cut test method according to *ASTM D3359-09, 2009*. The scratch hardness of the prepared dry films was estimated by using pencil hardness tester according to *ASTM D3363-05, 2011*. The bending of the prepared dry films was measured by cylindrical mandrel bending tester according to *ASTM D522-08, 2008*. The dried films, coated on tin plates, were bent over a cylindrical mandrel of different mm diameter and the resistance to cracking of the coatings was determined. The impact resistance test was estimated according to *ASTM D5420-10* with a falling weight of 1700 g at a height of 40 inches.

Visual corrosion test

Steel panels (5 × 7 cm² area) were coated with the prepared coating blends and left to dry for 1 week. The panels were edged with wax to prevent the attacking from the edges, and the coated faces were scratched with a sharp blade to 1-mm width to expose the bare metal. The panels were then exposed to artificial seawater (3.5 wt% NaCl solution) for 28 days. At the end of this time the panels were visually evaluated for the degree of rusting and degree of blistering according to *ASTM D 610-08, 2012* and *ASTM D 714-02, 2009*, respectively.

TABLE 1. Coating blends of emulsified resins loaded without and with different weight % of PANE.

Coating formulas	SACE (g)	PANE (g)	% PANI in the net coatings
F0	100	----	0
F0.5	98.60	1.40	0.5
F0.75	97.91	2.09	0.75
F1	97.23	2.77	1
F1.25	96.57	3.43	1.25
F1.5	95.91	4.09	1.5

**Fig. 2. The prepared coating formulas and PANE.**

Electrochemical corrosion measurements

The potentiodynamic polarization test was carried out by workstation Autolab PGSTAT302N – High-Performance potentiostat/galvanostat instrument. Three conventional electrode cells; a working CS electrode, a platinum counter electrode, and a reference Ag/AgCl electrode, were immersed in 3.5 % NaCl as an aggressive solution at room temperature. Tafel curves or potentiodynamic polarization curves of bare and coated CSs were measured from steady-state potential ± 250 mV at a scan rate of 2 mVs⁻¹. Corrosion rate information was obtained by the extrapolation of the Tafel plots which provides the cathodic and anodic polarization curves of the corrosion processes. Extrapolation of these curves to their point of intersection provides both the corrosion potential and the corrosion current density.

The electrochemical parameters were estimated as follows:

Corrosion current (I_{corr}) in amperes/cm² was

given according to Stern-Geary equation (1) [16]

$$I_{\text{corr}} = \frac{1}{R_p} \frac{\beta_a \beta_c}{2.303 (\beta_a + \beta_c)} \dots \dots \dots (1)$$

where R_p is the polarization resistance in ohm.cm², β_a and β_c are the anodic and cathodic tafels slopes in volts/decade, respectively.

Corrosion rate (CR) in millimeters per year (mm/y) was calculated from Faraday's law equation (2) [17]

$$CR = \frac{I_{\text{corr}} K. EW}{dA} \dots \dots \dots (2)$$

where K is a constant that defines the units of corrosion rate and equals to 3272 mm/y, EW is the equivalent weight in grams/equivalent, d is the density in g/cm³, A is sample area in cm².

The coating efficiency (η %) was calculated according to equation (3) [17]

$$\eta \% = \frac{I_{\text{corr}} - I_{\text{corr}}^0}{I_{\text{corr}}} \times 100 \quad (3)$$

where I_{corr} and I_{corr}^0 are the corrosion currents in the absence and the presence of the coating, respectively.

Weight loss measurement

The weight loss of bare and coated steel panels was determined by exposing the metal specimen of known area to a corrosive environment and following the loss in weight periodically according to *ASTM D2688-II, 2011*. The value of weight loss for a sample at a specific time is an average of three determinations.

The corrosion resistance efficiency ($E\%$) was calculated by the following relation:

$$E\% = \frac{W_0 - W}{W_0} \times 100$$

where W_0 is the weight loss of uncoated CS and W is the weight loss of coated CS.

The corrosion rate (CR) in mm/y (millimeter per year) was obtained from the following equation [18]:

$$CR = 87.6 \times \frac{W}{DAT}$$

where W is the weight loss of CS in mg, D is the metal density in g/cm^3 , A is the area of the sample, and T is the time of exposure of the metal sample in hours.

Results and Discussion

Analytical tests

The glass transition temperatures (T_g) of the coated films were estimated in their DSC curves presented in **Fig. 3**. The T_g of the coated films was indicated by the endothermic shifts in the DSC curves. It can be noticed an increase in the T_g of the coated films with an increased amount of PANI loaded in the SACE film. T_g increased from 23 °C for pure SACE film (F0), 27 °C for 0.5% loaded-PANI in the SACE matrix (F0.5), 28.9 °C for F0.75 film, 30.7 °C for F1 film, 32.2 °C for F1.25 film, to reach the maximum value at F1.5 film (36 °C). This general increase in T_g of the films after each uploading of PANI chains in the styrene-acrylate matrix could be attributed to the physical interactions generated between PANI chains and poly(styrene-co-butyl

acrylate) chains [19]. Such physical interactions, including H-bonds, *CH- π* , *polar- π* , *π - π* , and *Ar-Ar* interactions, restrict the segmental motions of the polymeric chains and raise the T_g of the film [20,21].

The particle size distribution curves of the prepared formulations are presented in **Fig. 4**. The neat styrene-acrylate emulsion (F0) showed a pure unimodal size distribution curve of a median P.S. ~158 nm. However, the entire SACE/PANE Fs exhibit bimodal distribution pattern at median P.S. of ~158 nm and ~48 nm related to SACE and PANE, respectively. The mean P.S. and the peak areas of the Fs and their % are listed in **Table 2**. There are a descending in the peak area values of SACE curves while an ascending in the values of PANE ones with increasing PANE added in the coating formulations. The peak area % of SACE decreased from 100% at F0 to reach the least at 98.33% for F1.5. However, an increase in the peak area % of PANE is observed from 0.55% for F0.5 to a maximum at 1.67% for F1.5. The peak areas percentages of PANE are very close to those of PANI in the net coatings listed in **Table 1**.

The SEM micrographs of F0 and F0.75 surface films are shown in **Fig. 5a and 5b**, respectively. The morphological structure of the F0 surface is smooth and clear. However, the surface of F0.75 is roughed by the inclusion of PANI chains within the styrene-acrylate copolymer matrix. The TEM photos of F0 and F0.75 coating formulations are presented in **Fig. 5c and 5d**, respectively. Clear spherical particles are shown in the TEM image of F0 representing the colloidal particles of SACE. The diameter of the particles is around 160 nm. However, the TEM image of F0.75 showed smaller spherical particles of diameter around 49 nm related to PANI particles besides the SACE particles. These data are in accordance with that obtained from DLS analysis.

Physical and mechanical properties

The physical properties of the prepared blended emulsions and the mechanical characteristics of the coated films are listed in **Table 3**. The S.C.% and viscosity decreased gradually with increasing the amount of PANE added to SACE. This is due to the lower S.C.% of PANE (18%) than SACE (51.1%). The density of the blended emulsions decreased in accordance with the reduction of

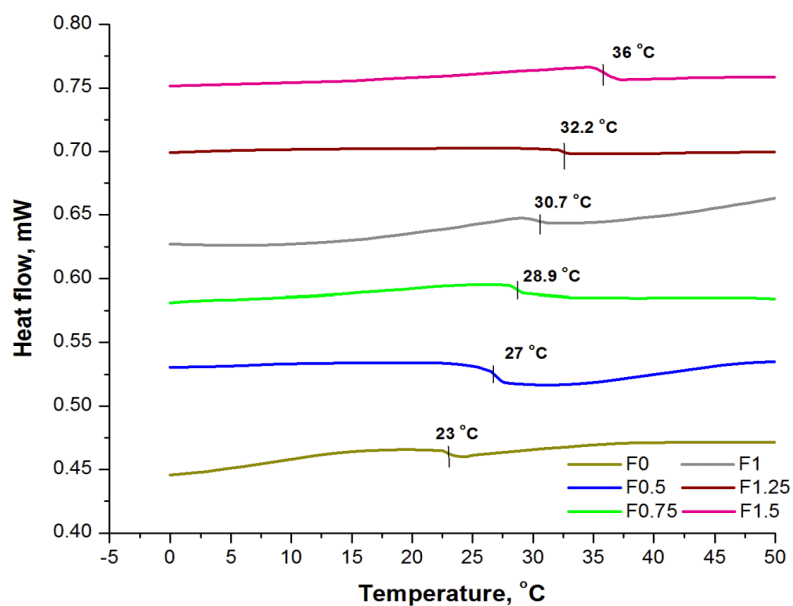


Fig. 3. DSC curves of the prepared Fs films.

TABLE 2. The mean particle size, peak area, and peak area % of the coating formulations.

Coating formulas	Mean P.S. (nm)		Peak area		Peak area %	
	SACE	PANE	SACE	PANE	SACE	PANE
F0	158	-----	2326	-----	100	-----
F0.5	158	48	2288	12.63	99.45	0.55
F0.75	158	48	2269	18.06	99.21	0.79
F1	158	48	2248	23.19	98.98	1.02
F1.25	159	48	2239	29.03	98.72	1.28
F1.5	160	48	2224	37.94	98.33	1.67

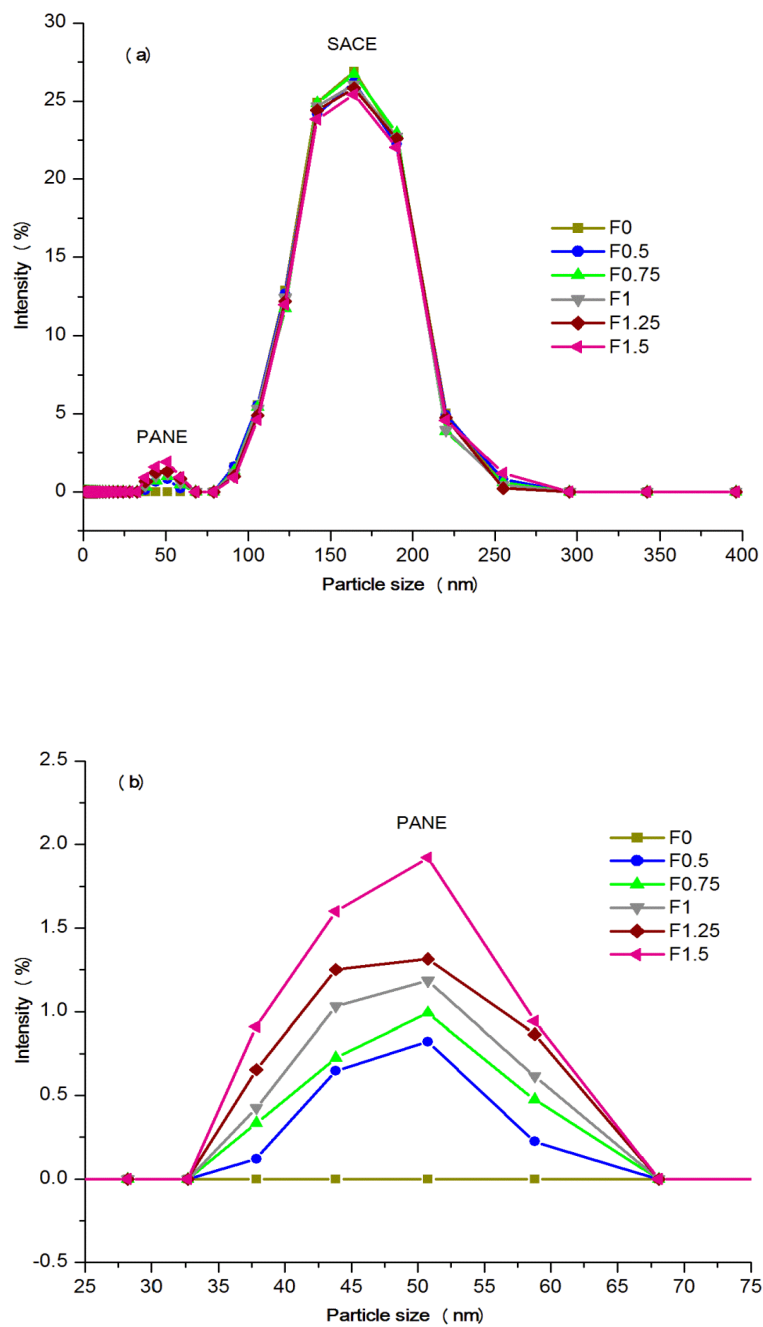


Fig. 4. Particle size distribution curves of Fs in the size range from (a) 0 to 600 nm and (b) 20 to 80 nm.

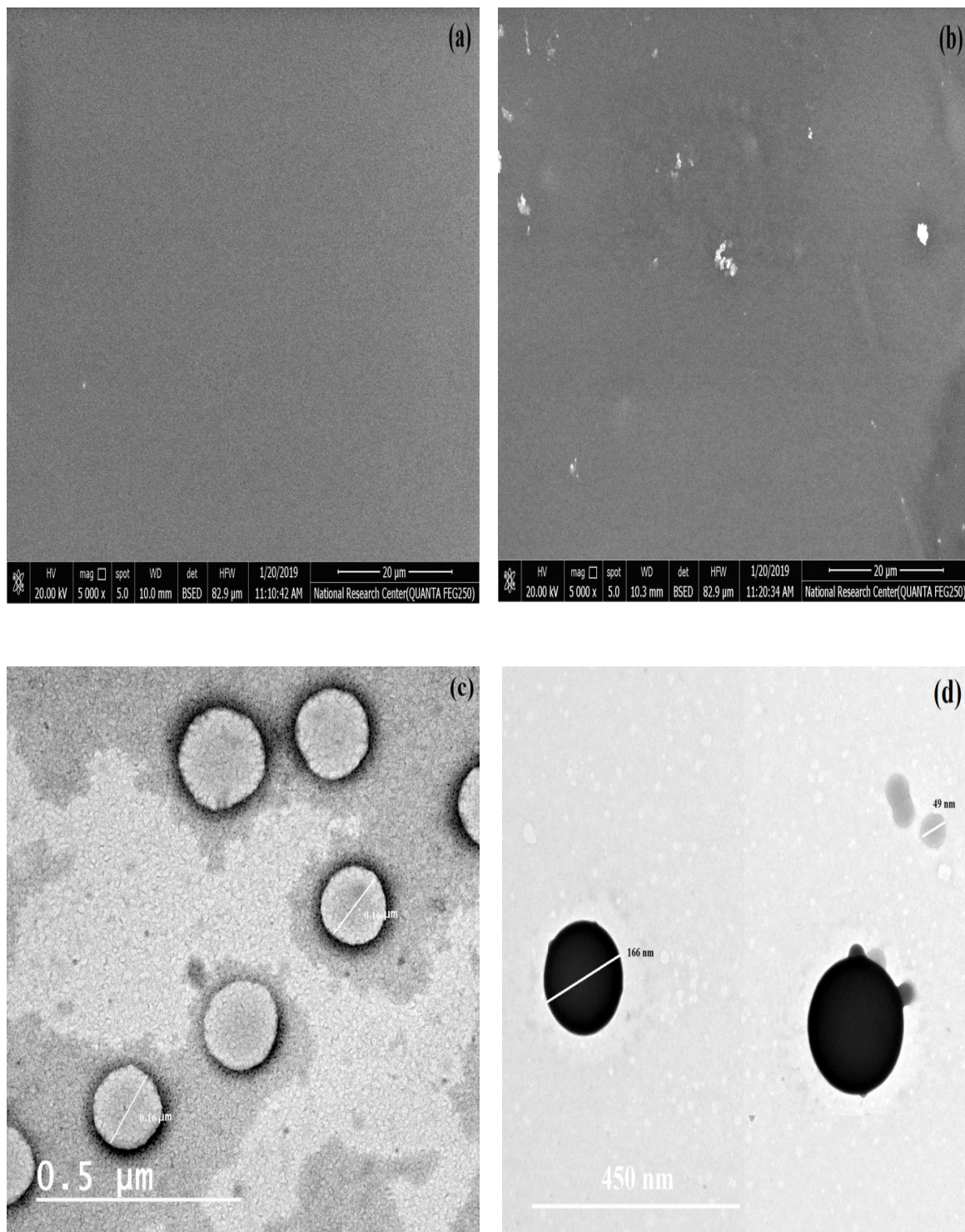


Fig. 5. SEM micrographs of (a) F0 and (b) F0.75 and TEM images of (c) F0 and (d) F0.75.

S.C.% and viscosity. Also, according to the results obtained from the DSC curves regarding the increase in the physical interactions between the polymeric chains, the flexibility of the films decreased and their hardness increased with increasing the amount of PANI in the films. In addition, the cross-cut adhesion decreased in the same direction due to the increase in the cohesive force at the expense of the adhesion to the substrate.

Visual Corrosion Test

The visual corrosion cross-cut test photos of the steel panels coated with Fs and immersed in 3.5% salt solution for 28 days are presented in **Fig. 6**. The images show at first glance that the F0.75, F1, and F0.5 coatings outperform the rest of the coatings in protecting the steel substrates from corrosion. The estimated values of the degrees of both rusting and blistering are listed in **Table 4**. The degrees of rusting and blistering were estimated to be the maximum at the steel

panels coated with F1.5 and F1.25. In the steel panels coated with formulations with lower PANI content, the corrosion product appears to be very little indicating good protection. Also, no blisters exist in steels coated with F0.5, F0.75, and F1.

Electrochemical corrosion measurements

Figure 7 shows the Tafel polarization plots of bare and coated CS in 3.5% NaCl solution. The electrochemical corrosion parameters of CS, F0, F0.5, F0.75, F1, F1.25, and F1.5 are listed in **Table 5**. It is clearly obvious that all the coated-CS plots are shifted to lower current density values. Also, their corrosion potentials are moved to a more positive direction compared with bare CS. This clarifies the protection behavior of the coated films as good barriers against the corrosive species in the medium. I_{corr} is lowered from $\sim 12 \mu\text{A}/\text{cm}^2$ for bare CS to $0.075 \mu\text{A}/\text{cm}^2$ for CS coated with F0.75 and rose up again to $0.687 \mu\text{A}/\text{cm}^2$ for F1.5-coated CS. The passivation effect of PANI was recorded by the increase in E_{corr} -0.63 V for bare CS to the less negative values for the

TABLE 3. Physical properties of the prepared coating formulations and the mechanical characteristics of their films.

Property	S.C. (%)	Viscosity (cp)	Density (g/cm ³)	Spreading rate (m ² /Kg)	Bending	Adhesion	Impact resistance	Hardness
F0	51.10	4565	1.1283	3.05	1 mm	5B	pass	F
F0.5	50.88	4495	1.1202	4.42	1 mm	5B	pass	H
F0.75	50.45	4465	1.1195	5.12	1 mm	5B	pass	H
F1	50.21	4386	1.1174	5.32	3 mm	5B	pass	2H
F1.25	50.13	4293	1.1088	6.88	6 mm	4B	pass	3H
F1.5	49.65	4173	1.1002	7.64	6 mm	3B	fail	4H

TABLE 4. The degree of rusting (DR) and the degree of blistering (DB) of the coated-films. (F: Few and MD: Medium Dense).

Coating formulations	DR	DB
F0	7	8F
F0.5	8	10
F0.75	9	10
F1	8	10
F1.25	3	4MD
F1.5	2	2MD

**F0****F0.5****F0.75****F1****F1.25****F1.5****Fig. 6.** Corrosion test of steel panels under the coated films.

coated-CSs [22]. This indicates that the PANI molecules appended anodic protection to the CS coated by the prepared formulations. Two factors directing the protection behavior of PANI; the first is the conductivity property of PANI chains which permits them to acquire electrons from the anodic CS surface and therefore oxidized. The second is their ability to be reduced again by the oxidative species such as H_2O and O_2 to regain their conductive structure [23,24].

Weight loss measurements

The weight loss measurements of bare-CS and coated-CS with the prepared formulations are shown in **Fig. 8**. Generally, the steel panels lost an increased weight with time due to the development of corroded areas generated by the electrochemical reaction of CS with O_2 , H_2O , and NaCl species in the medium. Bare CS exhibited the highest weight loss at all exposure times. However, F0.75-coated CS showed the least weight loss in accordance with the data obtained from the polarization curves. F1-coated CS demonstrated the maximum weight loss amongst all coated CSs. The protection efficiencies of the coatings and corrosion rate of CSs at different time intervals are extrapolated from the weight loss measurements and presented in **Table 6** and **Fig. 9**. The protection efficiency increased from 97.34%, respectively for F0-coated CS to

98.88% for F0.75-coated CS, and then descends gradually for F1-coated CS and sharply for F1.25-F1.5-coated CSs. The corrosion rate of the steel panels comes in reverse with the efficiency data where the highest protection gave the lowest corrosion rates. Therefore, F0.75-coated CS has the least corrosion rate at all time intervals due to the passivation effect of the PANI. However, the increased corrosion rates at higher PANI content give evidence of the increased intermolecular interactions. The binding between the F1.25 and F1.5 films and the steel substrate greatly decreased due to the increase of the cohesive forces. **Figure 10** presents a schematic illustration for the increased intermolecular interactions generated by the presence of high PANI content in the styrene-acrylate matrix. By the insertion of PANI chains, some physical bonds were added to the copolymer matrix through the benzenoid and quinoid rings in the PANI chains such as; *CH- π* and *polar- π* interactions between the copolymer and PANI chains and *π - π* and *Ar-Ar* interactions between either the copolymer and PANI chains or the same polymeric chains. These added physical interactions increased the cohesive force at the expense of the adhesion to the substrate. In addition, it changed the mechanical properties of the films as a whole.

TABLE 5. The corrosion parameters of CS in 3.5% NaCl solution in presence or absence of coated-films.

Sample	$-E_{corr}$	β_a (mV/dec)	$-\beta_c$ (mV/dec)	R_p ($\Omega.cm^2$)	I_{corr} (nA/ cm^2)	$CR \times 10^{-4}$ (mm/Y)	η %
CS	637.25	53.83	18.82	508	11926	413.67	-----
F0	547.34	4.280	10.97	6964	192.00	5.16	98.39
F0.5	541.43	5.686	8.724	10185	146.76	4.018	98.77
F0.75	568.35	3.673	6.809	13794	75.110	1.92	99.37
F1	554.20	4.793	6.851	11124	110.09	3.65	99.06
F1.25	561.29	5.211	6.157	3241	378.11	8.025	96.83
F1.5	555.58	8.816	10.84	3071	687.44	12.74	94.23

TABLE 6. The efficiencies of the coating blends estimated from weight loss measurements.

Sample	E % (10 days)	E % (20 days)	E % (30 days)	E % (40 days)	E % (50 days)	E % (60 days)	E % (Average)
F0	97.43	97.10	97.21	97.32	97.41	97.55	97.34
F0.5	98.02	97.91	98.05	98.05	98.01	98.22	98.04
F0.75	98.87	98.75	98.92	98.95	98.94	98.83	98.88
F1	98.43	98.52	98.34	98.67	98.75	98.55	98.55
F1.25	95.67	95.72	95.20	95.33	95.37	95.66	95.49
F1.5	92.51	92.22	92.44	92.35	92.56	92.72	92.47

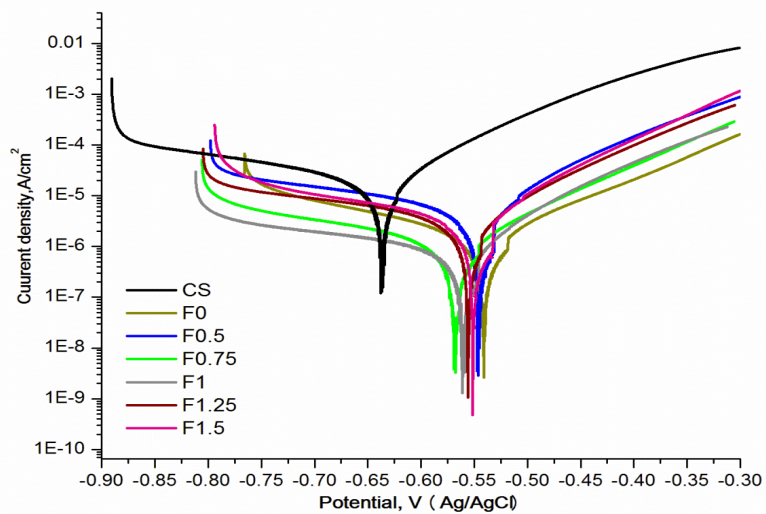


Fig. 7. Tafel polarization curves of CS, F0, F0.5, F0.75, F1, F1.25, and F1.5 in 3.5% NaCl solution.

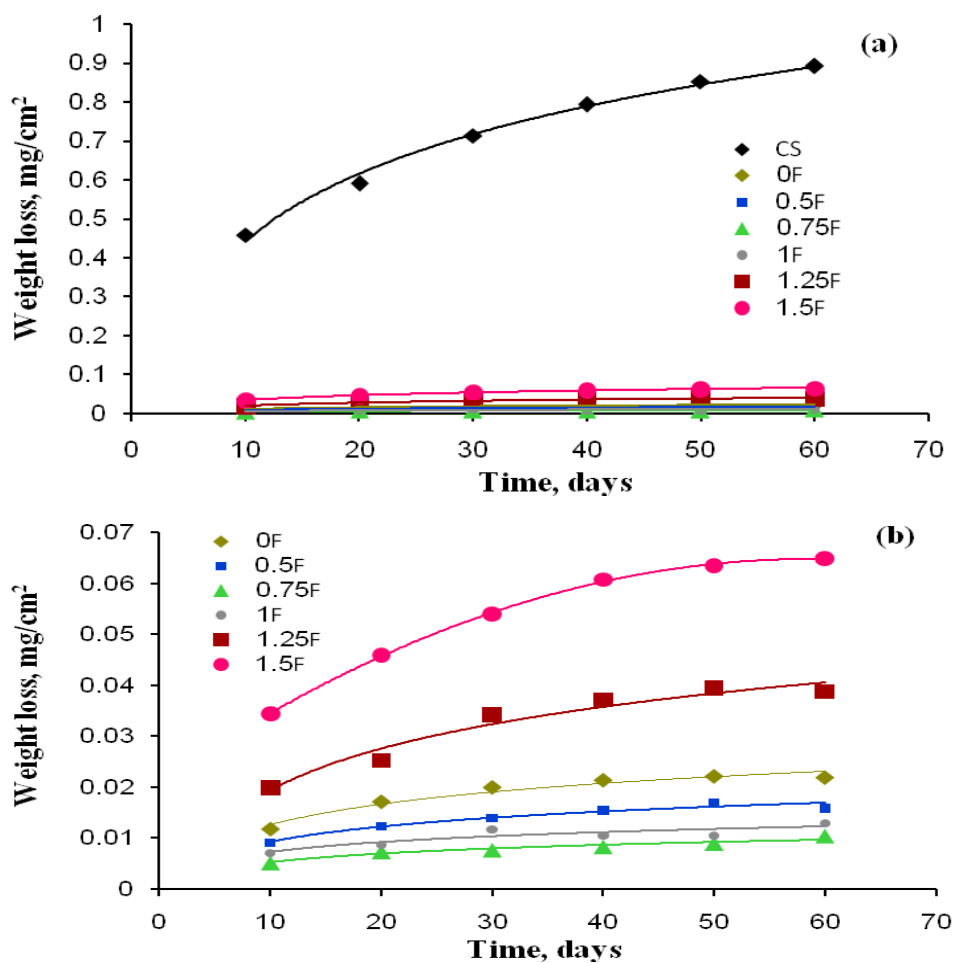


Fig. 8. Weight loss measurements of CS, F0, F0.5, F0.75, F1, F1.25, and F1.5 (a) and enlarged figure of F0, F0.5, F0.75, F1, F1.25, and F1.5 (b).

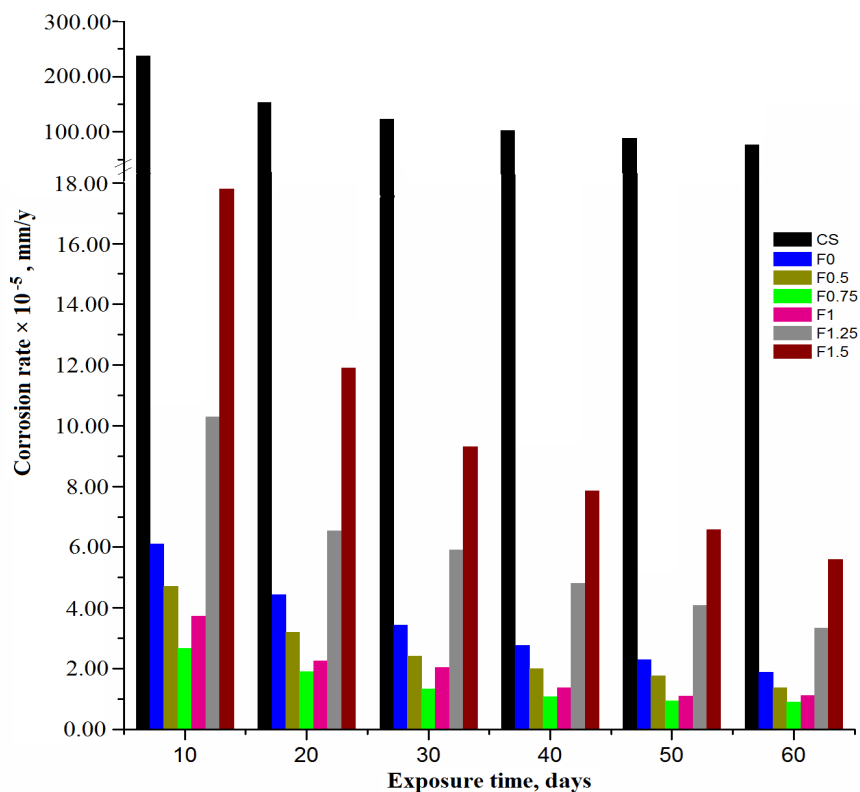


Fig. 9. Corrosion rate measurements of CS, F0, F0.5, F0.75, F1, F1.25, and F1.5 at different exposure times.

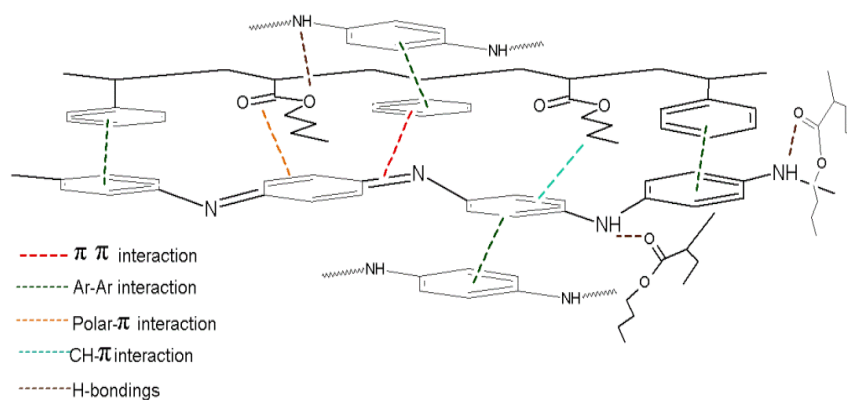


Fig. 10. A suggested molecular structure of the copolymer/PANI including the intermolecular interactions generated by the increased amount of PANI in the styrene-acrylate matrix.

Conclusion

Poly (styrene-*co*-butyl acrylate) and PANI emulsions were prepared and blended to give eco-friendly coating formulations with different solid to solid ratios. The blended formulations showed bimodal size distribution patterns related to the PANI and copolymer particles. The coated films were used to protect the steel substrate against corrosion. The T_g of the films

increased progressively with the PANI content. Coating films loaded with 0.75% and 1% PANI exhibited the optimum corrosion resistivity and their efficiencies were 99.37% and 99.06%, respectively. However, at higher concentrations, the intermolecular forces increased and the adhesion to the steel substrate greatly decreased. The passivation effect of PANI was confirmed by the shift in the potential to the anodic direction.

References

1. Mohamed H.A., Morsi S.M.M., Badran B.M., Rabie A.M., Eco-friendly protective coatings based on poly(urethane sulfone amide) dispersions for carbon steel, *Journal of Coatings Technology and Research*, **14**, 437–446 (2017).
2. Abd El-Ghaffar M.A., Baraka A.M., Hefny M.M., Youssef E.A., Aly M.M., Boron Phosphate/Poly(p-phenylenediamine) as a Corrosion Inhibitive System for Steel Protection, *Egyptian Journal of Chemistry*, **61**, 759-771 (2018).
3. Zaky M.F., Sabbah I.A., Negm N.A., Hendawy M.E., Biocidal Activity and Corrosion Inhibition of Some Cationic Surfactants Derived from Thiol Polyurethane, *Egyptian Journal of Chemistry*, **61**, 45-60 (2018).
4. Olad A., Naseri B., Preparation, characterization and anticorrosive properties of a novel polyaniline/clinoptilolite nanocomposite, *Progress in Organic Coatings*, **67**, 233–238 (2010).
5. Mostafa H.Y., Hussain A.I., El-Masry A.M., Maher A., Novel Core–Shell of Polymethyl Methacrylate/butyl Acrylate/vinyl Silica Nanocomposite Particles through Seed Emulsion Polymerization, *Polymer - Plastics Technology and Engineering*, **56**, 411-420 (2017).
6. Hussain A.I., Aly A.A., Zakaria N., Saleh A., Novel Maleate Surfmer for Stabilization High-solid Content of Methyl Methacrylate/Butyl Acrylate Copolymer Emulsion System, *Polymer - Plastics Technology and Engineering*, **11**, 1203-1212 (2017).
7. Mohsen R.M., Morsi S.M.M., Abu-Ayana Y.M., Ghoneim A.M., Synthesis of conductive Cu-core / Ag-subshell / polyaniline-shell nanocomposites and their antimicrobial activity, *Egyptian Journal of Chemistry*, **61**, 590-600 (2018).
8. Mohsen R.M., Morsi S.M.M., Selim M.M., Ghoneim A.M., El-Sherif H.M., Electrical, thermal, morphological, and antibacterial studies of synthesized polyaniline/zinc oxide nanocomposites, *Polymer Bulletin*, **76**, 1-21 (2019).
9. Boeva Z.A., Sergeev V.G., Polyaniline: Synthesis, Properties, and Application, *Polymer Science Series C*, **56**, 144–153 (2014).
10. Palaniappan S., John A., Polyaniline materials by emulsion polymerization pathway, *Progress in Polymer Science*, **33**, 732–758 (2008).
11. Lamouri S., Zeghina S., Polyaniline/Styrene-Acrylic acid copolymer system: Thermic and electric Characterization, *Journal of Nanostructured Polymers and Nanocomposites*, **4**, 94-99 (2018).
12. Wu L., Ge Y., Zhang L., Yu D., Wu M., Ni H., Enhanced electrical conductivity and competent mechanical properties of polyaniline/polyacrylate (PANI/PA) composites for antistatic finishing prepared at the aid of polymeric stabilizer, *Progress in Organic Coatings*, **125**, 99-108 (2018).
13. Mirmohseni A., Gharieh A., Khorasani M., Waterborne acrylic–polyaniline nanocomposite as antistatic coating: preparation and characterization, *Iranian Polymer Journal*, **25**, 991-998 (2016).
14. Morsi S.M.M., Abd El-Aziz M.E., Morsi R.M.M., Hussain I., Polypyrrole-coated latex particles as core/shell composites for antistatic coatings and energy storage applications, *Journal of Coatings Technology and Research* **16**, 745–759 (2019).
15. Plesu N., Liescu S., Illa G., Popa A., Muntean C., Rheology of Polyaniline Dispersions in Acrylic Resin, *Turkish Journal of Chemistry*, **30**, 155-163 (2006).
16. Stern M., A Method For Determining Corrosion Rates From Linear Polarization Data, *Corrosion*, **14**, 60-64 (1958).
17. Morsi S.M.M., Emira H.S., El-Sawy S.M., Mohsen R.M., Khorshed L.A., Synthesis and characterization of kaolinite/polyaniline nanocomposites and investigating their anticorrosive performance in chlorinated rubber/alkyd coatings, *Polymer Composites* **40**, 2777-2789 (2019).
18. Nwankwo M.O., Nwobasi P.A., Offor P.O., Idenyi N.E., Unification of the Quadratic Model Equations of the Inhibition Characteristics of Acidified Ocimum Basilicum on the Corrosion Behaviour of Mild Steel, *Journal of Minerals and Materials Characterization and Engineering*, **1**, 367-373 (2013).
19. Lamouri S., Zeghina S., Polyaniline/Styrene-Acrylic acid copolymer system: Thermic and electric Characterization, *Journal of Nanostructured Polymers and Nanocomposites*, **4**, 94-99 (2018).
20. Morsi S.M.M., Mohamed H.A., A comparative study of new linear and hyperbranched polyurethanes built up from a synthesized isocyanate terminated polyester/urethane, *Polymer Bulletin*, **74**, 5011–5027 (2017).
21. Morsi S.M.M., Mohamed H.A., El-Sabbagh S.H.,

- Polyesteramidesulfone as novel reinforcement and antioxidant nanofiller for NBR blended with reclaimed natural rubber, *Materials Chemistry and Physics*, **224**, 206–216 (2019).
22. Sekunowo O.I., Adeosun S.O., Lawal G.I., Potentiostatic Polarisation Responses Of Mild Steel In Seawater And Acid Environments, *International Journal of Scientific & Technology Research*, **2**, 139-145 (2013).
23. Gvozdenovic M., Jugovic B., Jambrec D., Stevanovic J., Grgur B., Application of polyaniline in corrosion protection of metals, *Journal Materials Protection*, **53**, 353-360 (2012).
24. Ohtsuka T., Corrosion Protection of Steels by Conducting Polymer Coating, *International Journal of Corrosion*, **215**, 1-7 (2012).

مستحلب البولوي أنيلين كمثبط في طلاءات الستيرين - أكريلات المائية لحماية الصلب الكربوني ضد التآكل

سمير مرسى محمد^١، لبنى عبد العزيز فؤاد خورشيد^٢، جورجينا نبيل سمعان^٣، سامية صبحي يونس^٤، إيهاب فؤاد أبادير^٥، أحمد اسماعيل حسين^٦

^١قسم البلمرات و المخضبات - المركز القومي للبحوث - الجيزة - مصر.

^٢قسم الكيمياء الفيزيائية - المركز القومي للبحوث - الجيزة - مصر.

^٣وكالة التجارة الدولية والتسويق (اتامكو) - القاهرة - مصر.

^٤قسم الهندسة الكيميائية - كلية الهندسة - جامعة القاهرة - الجيزة - مصر.

في هذا البحث تم الاستفادة من التأثير التخميلى للبولوي أنيلين لتعزيز كفاءة الحماية لطلاءات الستيرين-أكريلات المائية ضد تآكل الصلب الكربوني. فقد تم تحضير مستحلب الستيرين - أكريلات المرتكز على بوليمر مشترك من (ستيرين - بيوتيل أكريلات) عن طريق بلورة الاستحلاب بينما تم تحضير مستحلب البولوي أنيلين بواسطة بلورة الأكسدة الكيميائية للأنيلين في كريات الصوديوم دوديسيل بنزين سلفونات الاستحلابية. أما تركيبات الطلاء فقد حضرت بإضافة مستحلب البولوي أنيلين إلى مستحلب الستيرين - أكريلات بنسب وزنية مختلفة. و قد تمت دراسة اللزوجة و الكثافة و المحتوى الصلب و توزيع حجم الجسيمات و شكلها و ثبات المستحلبات المخلوطة. و قيمت خصائص أفلام الطلاءات من حيث الصلابة و مقاومة الصدمات و المرونة و قوة الالتصاق بالصلب و درجة حرارة التحول الزجاجي و مورفولوجيا السطح. كما تم تقييم تأثير مستحلب البولوي أنيلين في تعزيز كفاءة حماية أفلام مستحلب الستيرين - أكريلات ضد تآكل الصلب الكربوني من خلال اختبار تآكل ألواح الصلب المطلية بالغمر في محلول ملحي تركيزه ٣,٥٪ كلوريد الصوديوم، وقياسات الفقد في الوزن، و كذلك القياسات الكهروكيميائية كالإستقطاب البوتنشيو ديناميكي (معدل التآكل، جهد التآكل، مقاومة الاستقطاب). و قد أظهرت النتائج زيادة في درجة حرارة التحول الزجاجي من ٢٣ درجة سيلوليوزية لفيلم الستيرين - أكريلات ليصل إلى ٣٦ درجة سيلوليوزية لفيلم الستيرين - أكريلات الذي يحتوي على أكثر كمية من البولوي أنيلين. كما أظهر فيلم الستيرين - أكريلات المحمل بـ ٠,٧٥٪ و ١٪ من البولوي أنيلين أقل كثافة لتيار التآكل ممكنة و ذلك نتيجة تكون طبقة واقية وحامية للصلب الكربوني والتي أدت بدورها إلى إزاحة قيمة جهد التآكل إلى الإتجاه الموجب.